Galactose-functionalized dendritic siRNA-nanovector to potentiate hepatitis C inhibition in liver cells

Abirami Lakshminarayanan[1,2], B. Uma Reddy[2], Nallani Raghav[3], Vijay Kumar Ravi[3], Anuj Kumar[2], Prabal K. Maiti[*3], A. K. Sood[*3], N. Jayaraman[*1], Saumitra Das[*2],

[1]Department of Organic Chemistry, [2]Department of Microbiology and Cell Biology, [3]Department of Physics; Indian Institute of Science, Bangalore 560012, India.

Address for correspondence:

Prof. Saumitra Das: sdas@mcbl.iisc.ernet.in

Prof . N. Jayaraman: jayaraman@orgchem.iisc.ernet.in

Prof. A. K. Sood: asood@physics.iisc.ernet.in

Prof. Prabal K. Maiti: maiti@physics.iisc.ernet.in

Materials. All chemicals for synthesis, and biological assays were purchased from Sigma-Aldrich, India unless mentioned otherwise. siRNAs, siRNA buffer, primers, enzymes and real time PCR kit were procured from Thermo Fischer Scientific Inc. India. The media for cell culture was purchased from Sigma Aldrich, India; while serum and Lipofectamine 2000 were purchased from Invitrogen, India.
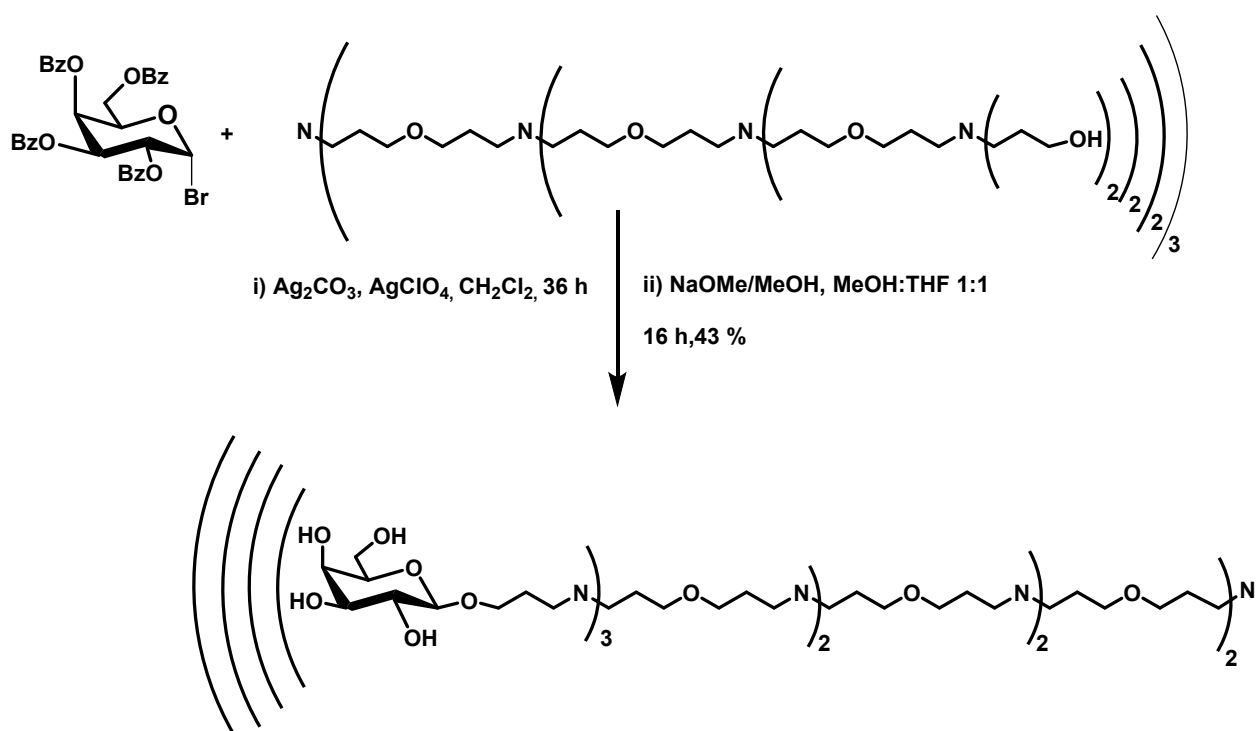
Figure S1. Synthesis of galactose functionalized PETIM dendrimer. Third generation hydroxyl functionalized PETIM dendrimer was glycosylated with tetra per-*O*-benzoyl galactosyl bromide followed by deprotection of benzoyl groups to yield DG.
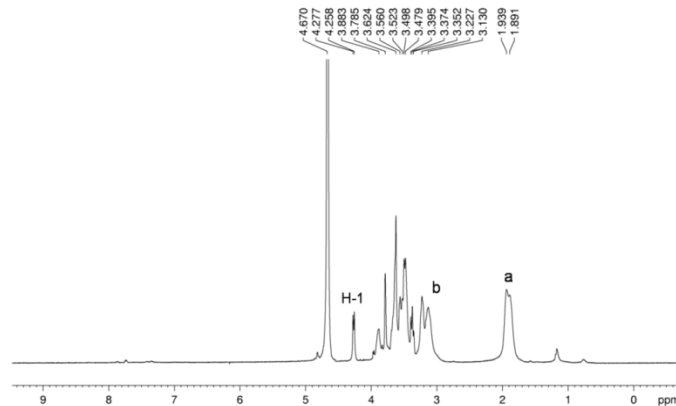
Figure S2. ^{1}H NMR of DG in D_2O, 400 MHz. The peak labeled 'a' correspond to the dendrimer protons, CH_2-CH_2-CH_2; 'b' corresponds to CH_2-CH_2-N-CH_2-CH_2 protons of the dendrimer while H-1 denotes the anomeric protons from the galactose units attached to the dendrimer.
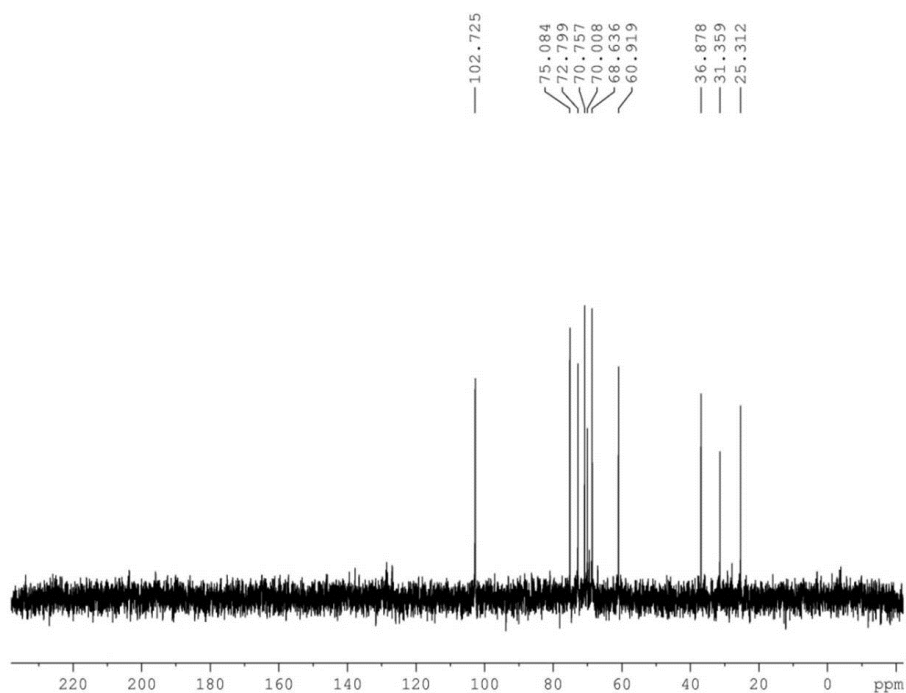
**Figure S3.** ^{13}C NMR of DG in D_2O, 100 MHz. The anomeric carbon peak at 102.7 ppm confirms the α-orientation galactose units attached to the dendrimer.

3

Procedure for the phenol-H$_2$SO$_4$ assay. To a solution of 20 µL of the DG (or D-galactose) in a U-shaped well of a 96-well microtiter plate, 20 µL of a 6 mg mL^{-1} solution of phenol and 100 µL of concH$_2$SO$_4$were added. The solutions were homogenized by vigorous pipeting to ensure complete mixing. The plates were heated at 90 ^{o}C for 30 min. and subsequently kept at room temperature for 45 min. in the dark. The absorbance of the solutions was recorded at 430 nm. The concentration of galactose units in DG was determined from the calibrated curve of absorbance *vs* concentration derived from a solution of D-galctose taken as the standard.
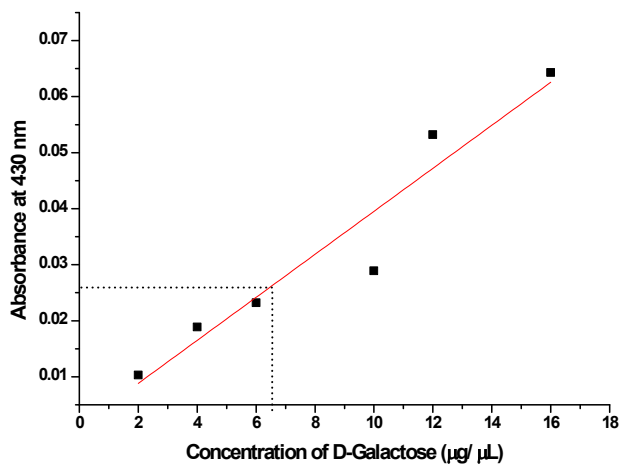

Figure S4. Calibration curve of the phenol-sulphuric acid assay. The dotted line indicates the absorbance obtained for the DG sample and hence the corresponding concentration.

Gel retardation assay. siRNA (siGLO, 10 nM) and its complexes with DG (19 μM, 38 μM, 58 μM, 77 μM, 96 μM, 116 μM) corresponding to weight ratios (R) of 10, 20, 30, 40, 50, 60 were prepared in siRNA buffer and their complex forming ability was determined by gel electrophoresis. The gradual retardation and disappearance of the siRNA band indicated the formation of an electrostatic complex between the dendrimer and siRNA (Fig. S5). The significant decrease in fluorescence intensity and the disappearance of the bands beyond R 30 indicate loss of accessibility of siRNA to ethidium bromide binding due to complexation with dendrimer.
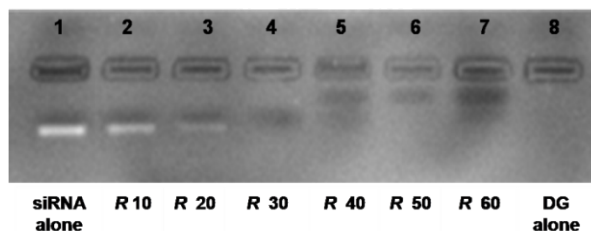
Figure S5. Gel retardartion assay for the siRNA-DG complexes at varying weight ratios; R 10, 20, 30, 40, 50, 60. The amount of siRNA in each of the complexes was 10 nM.The complexes were prepared in siRNA buffer (1X) and electrophoresed through a 2% formaldehyde-agarose gel at 100 V for 5 min.
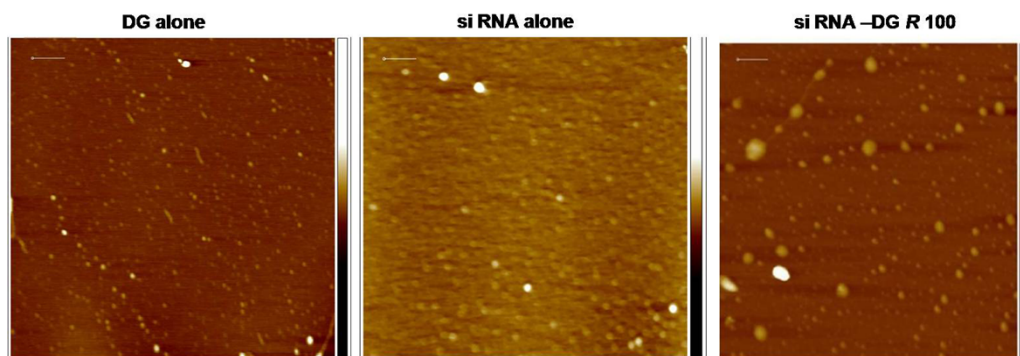
Figure S6. AFM images of dendrimer (DG), siRNA and the siRNA- DG complexes at R 100

Simulation details:

The beta galactose structure is Gaussian optimized with HF 6-31g basis set. Using antechamber module of AMBER, the RESP charges are calculated and GAFF atom types are assigned.[1] For the protonated case of the dendrimers the tertiary amines of the penultimate residue of the dendrimer is protonated as it is known from experiments that pKa of the galactose is much less than that of amine group. The galactose terminated PETIM dendrimer of generation 3 and 4 was built using Dendrimer builder toolkit (DBT).[2] The DBT built structure was solvated in TIP3P water using xleap module of AMBER 12[3] and was equilibrated for 20-30 ns in NPT ensemble using PMEMD software.[4] The equilibrated G3 dendrimer (both the protonated and non-protonated) was placed in the major groove and minor groove of siRNA. ff99bsc0[5] with parmbsc0 correction[6] was used to describe inter and intra molecular interaction involving siRNA molecule. The siRNA and dendrimer complex is solvated using xleap keeping a buffer of 15Å on all sides. The water model TIP3P[7] is used for solvation. The non-protonated dendrimer and siRNA requires only siRNA to have counter-ions to charge neutralize the system. In non-protonated cases the system is charge neutralized with 40 Na+ ions. In the protonated case the system is charge neutralized with 12 Cl- ions or 24 Cl- ions for the G3 or G4 dendrimer and 40 Na+ ions for the siRNA. The details of the simulated systems are given in table S1. The system was then energy minimized for 1000 steps using steepest descent method and further 2000 steps by conjugate gradient method. During the minimization, the solute was held fixed using harmonic constraint with a spring constant of 500 kcal/mol/Å^2, to eliminate bad contacts with solvent. Further 3000 steps of conjugate gradient minimization is carried out reducing the harmonic constraint by 5 kcal/mol/Å^2 at every 600 steps from 20 kcal/mol/Å^2 to 0 kcal/mol/Å^2. Then 40 ps of equilibration in NPT was performed heating the system from 0 K to 300 K.

Finally, 50 ns of production run in NVT ensemble was carried out. All the simulations were carried out using PMEMD[4] module of AMBER 12.

Table S1: Details of simulated systems.

Complex	#siRNA atoms	#dendrimer atoms	#of Na+ atoms	# of Cl- atoms	# water molecules	Total number of atoms
siRNA+G3P	884	1201	40	12	24326	75570
siRNA+G3NP	884	1189	40		20696	64656
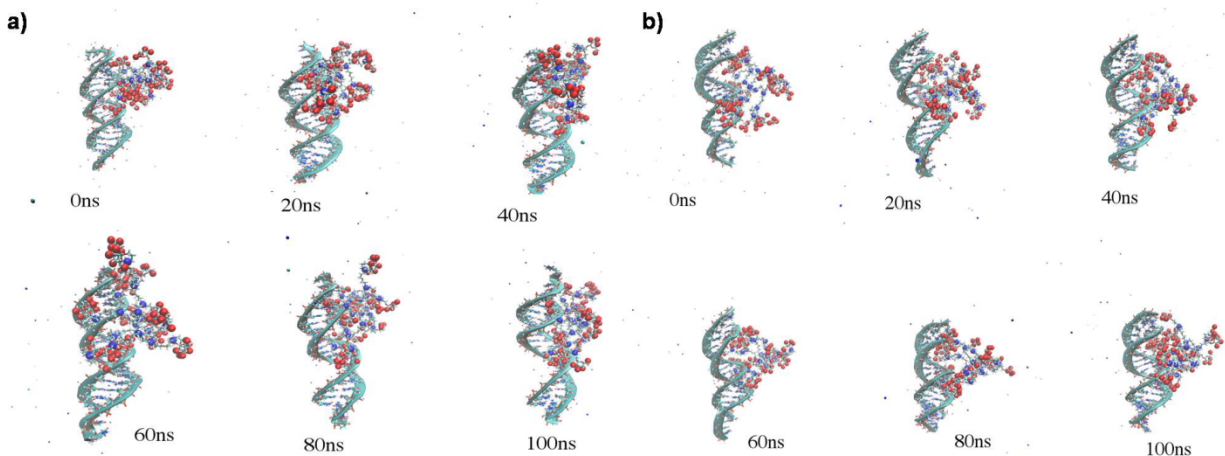
Figure S7. (a) Panel showing instantaneous snapshots of DG-siRNA complex from a 100ns simulation, where the protonated dendrimer is initially placed near the major groove. (b) Panel showing instantaneous snapshots of DG-siRNA complex from a 100ns simulation, where the protonated dendrimer is initially placed near the minor groove. The dendrimer being protonated is spread out through the major and minor grooves, but the major groove preference can be seen in both cases (a) and (b)
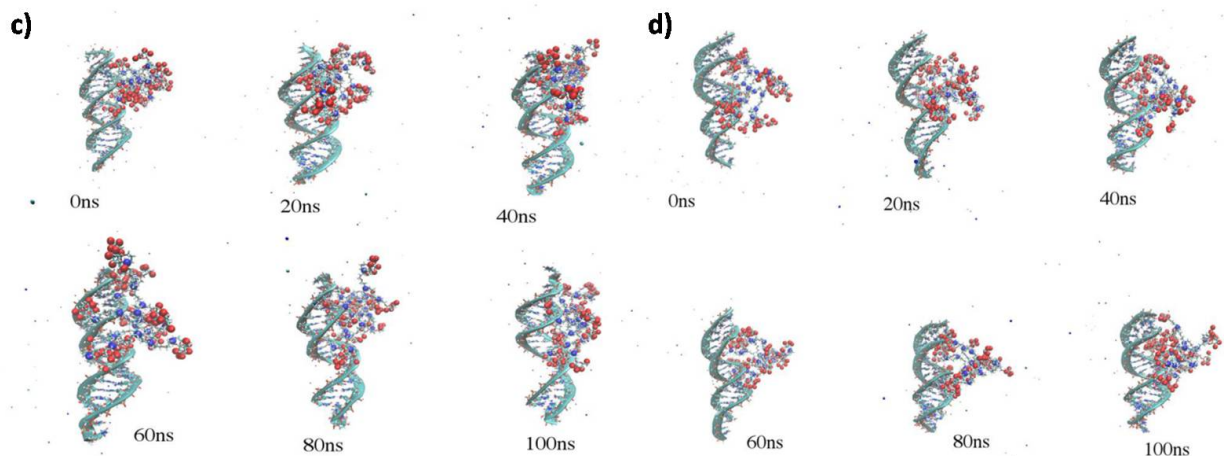
Figure S7. (c) Panel showing instantaneous snapshots of DG-siRNA complex from a 100ns simulation, where the protonated dendrimer is initially placed near the major groove. (d) Panel showing instantaneous snapshots of DG-siRNA complex from a 100 ns simulation, where the protonated dendrimer is initially placed near the minor groove. The dendrimer being protonated is spread out through the major and minor grooves, but the major groove preference can be seen in both cases (a) and (b)

The g(r) of the amine as well as sugar groups of dendrimer and phosphates of siRNA were studied by MD simulation. In Figure S8a, we plot the radial distribution of the nitrogen of the primary amine group and phosphate of the siRNA backbone. We see that when dendrimer is non-protonated, there is almost no coordination of the nitrogen of the amine and phosphate as is evident from the very low peak height of g(r). In contrast, for protonated dendrimer, the prominent first peak clearly demonstrates strong complexation between the dendrimer and siRNA. Similar feature we see while plotting the g(r) between the oxygen of galactose sugar and phosphate of siRNA as shown in Figure S8b.
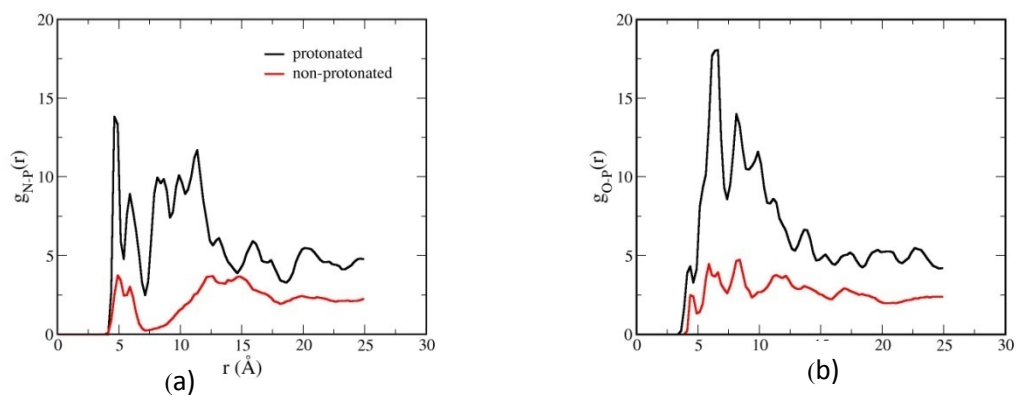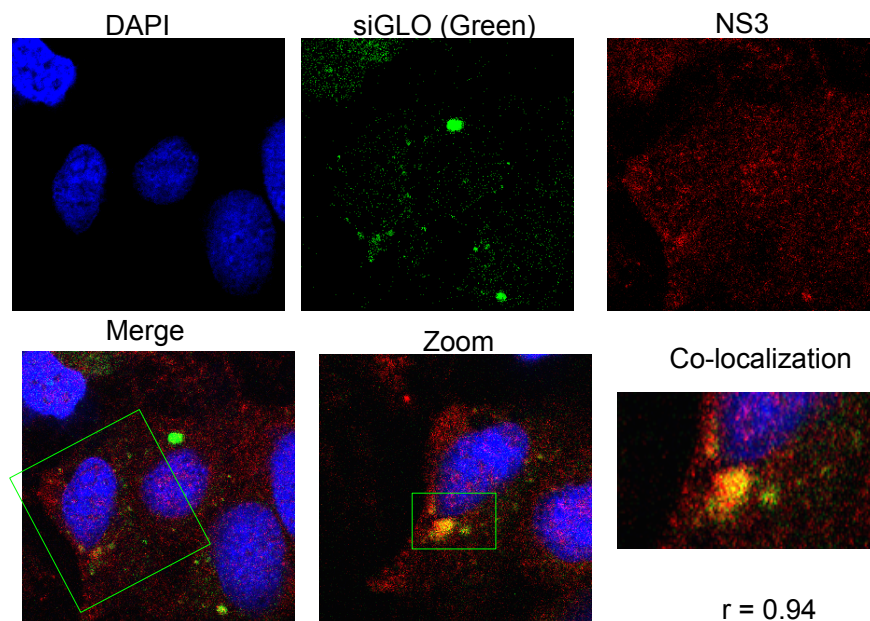
Figure S8. Radial distribution function between (a) the nitrogen of amine group of dendrimer and phosphate of siRNA. (b) the oxygen of galactose sugar and phosphate of siRNA.
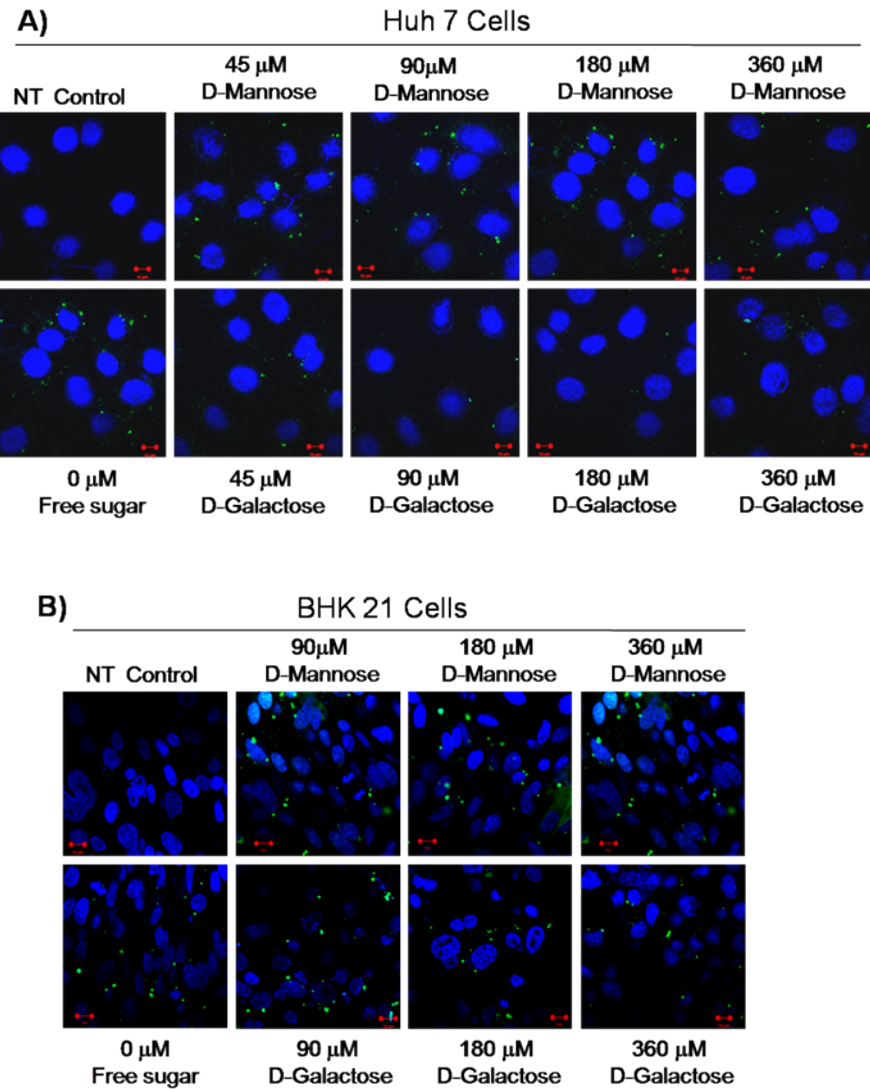
Figure 9. Confocal microscopy to showing the internalization of siGLO (green) in (A) Huh 7 cells and (B) BHK 21 cells at 45-360 µM concentrations of D-Galactose and D-mannose.

Figure S10. Colocalization of siRNA (siGLO, green) with HCV protein NS3 (labeled red) which is a part of virus replication complex. Co-localization coefficient was calculated to be 0.94. The nuclei are stained with DAPI.
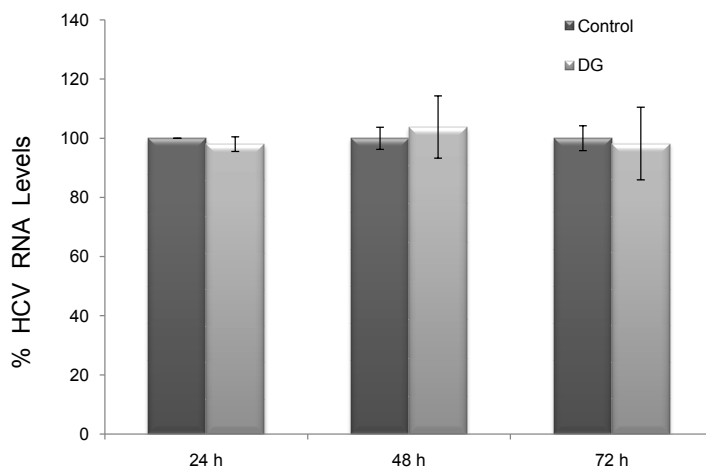

Figure S11. Levels of HCV RNA in Huh 7 cells harbouring HCV replicon transfected with DG alone. No changes in the HCV RNA levels with respect to control cells indicate that DG does not interfere with the replication of HCV RNA.

MTT assay. In a 96 well plate, 5×10^3 cells were seeded and allowed to grow for 16 h at 37 °C under 5% CO_2 conditions. The medium in the wells was then replaced with fresh medium, increasing concentrations of dendrimer added, and further the plate was incubated for 24 h at 37 °C in presence of 5% CO_2. 20 μL of MTT reagent (5 mg mL^{-1}) was then added into the wells and kept for 4 h in dark at 37 °C. The resultant formazone crystals were dissolved in 100 μL of DMSO (dimethyl sulfoxide) and the absorbance was recorded at 570 nm. Untreated cells were used as controls. The results represent an average of three such experiments in duplicates.
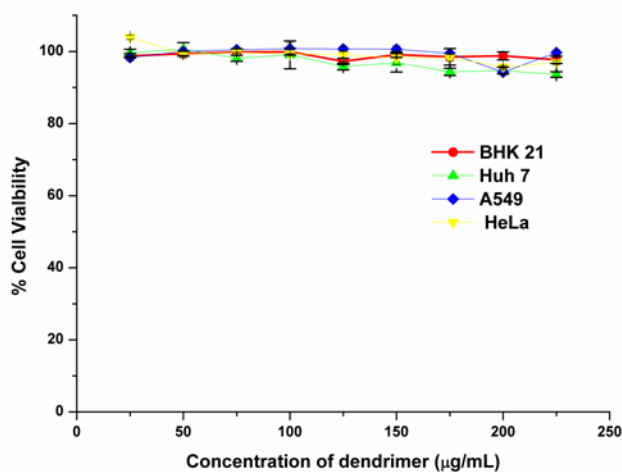
Figure S12. MTT assay of DG in different mammalian cell lines; Huh 7 (liver cells), BHK 21 (kidney cells), A549 (lung carcinoma cells), HeLa (cervical cancer cells). DG is completed non-toxic upto the tested concentration of 225 μg mL^{-1} in these cell lines.
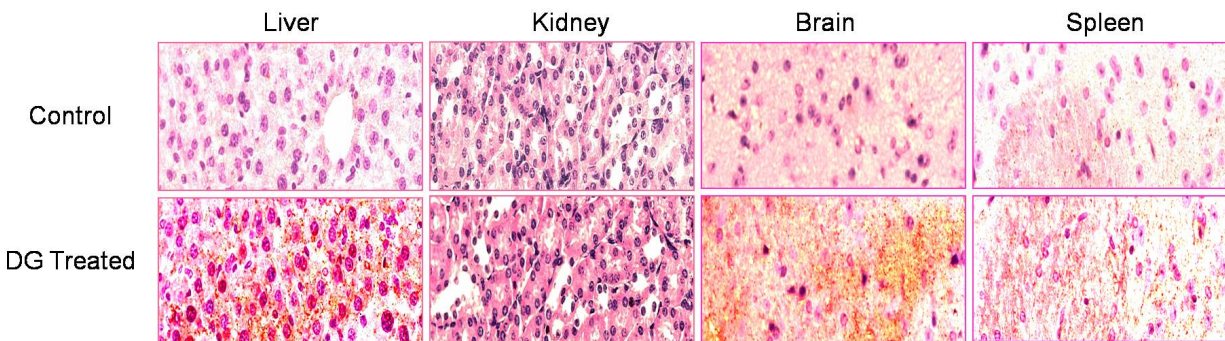
Figure S13. Immunohistochemistry (IHC) studies of mice tissues : liver, kidney, brain and spleen; isolated form mice treated with the galactose functionalized dendrimer DG. The brown precipitate indicated the luciferase production, probed using horse raddish peroxidase (HRP) reaction with luciferase primary antibody.

References

1. J. M. Wang, R. M. Wolf, J. W. Caldwell, P. A. Kollman and D. A. Case, *J. Comput. Chem.*, 2004, **25**, 1157-1174.

2. V. Maingi, V. Jain, P. V. Bharatam, and P. K. Maiti, *J. Comput. Chem.* 2012, **33**, 1997-2011.

3. D. A. Case, T. A. Darden, T. E. Cheatham, III, C.L. Simmerling, J. Wang, R. E. Duke, R. Luo, R. C. Walker, W. Zhang, K. M. Merz, B. Roberts, S. Hayik, A. Roitberg, G. Seabra, J. Swails, A.W. Götz, I. Kolossváry, K. F. Wong, F. Paesani, J. Vanicek, R. M. Wolf, J. Liu, X. Wu, S. R. Brozell, T. Steinbrecher, H. Gohlke, Q. Cai, X. Ye, J. Wang, M.-J. Hsieh, G. Cui, D.R. Roe, D.H. Mathews, M.G. Seetin, R. Salomon-Ferrer, C. Sagui, V. Babin, T. Luchko, S. Gusarov, A. Kovalenko, and P.A. Kollman (2012), AMBER 12, University of California, San Francisco.

4. R. Salomon-Ferrer, A. W. Goetz, D. Poole, S. L. Grand, and R. C. Walker, *J. Chem. Theory Comput.*, 2013, **9**, 3878.

5. J. Wang, P. Cieplak and P. A. Kollman, *J. Comput. Chem.*, 2000, **21**, 1049-1074.

6. A. Perez, I. Marchan, D. Svozil, J. Sponer, T. E. Cheatham III, C. A. Laughton and M. Orozco, *Biophys. J.*, 2007, **92**, 3817-3829.

7. W. L. Jorgensen, J. Chandrasekhar, J. D. Madura, R. W. Impey and M. L. Klein, *J. Chem. Phys.*, 1983, **79**, 926-935.